ISBN: 978-3-95450-184-7 doi:10.18429/JACoW-IPAC2018-WEPMF089

MEASUREMENTS OF ELECTROMAGNETIC PROPERTIES OF FERRITES AS A FUNCTION OF FREQUENCY AND TEMPERATURE

A. Chmielińska[1,*], B. Popovic, M. J. Barnes, F. Caspers, C. Vollinger, CERN, Geneva, Switzerland
[1] also at EPFL, Lausanne, Switzerland

Abstract

Fast kicker magnets are used to inject beam into and extract beam out of the CERN accelerator rings. These kickers are often ferrite loaded transmission line type magnets with a rectangular shaped aperture through which the beam passes. The interaction of the beam with the resistive part of the longitudinal beam coupling impedance leads to power dissipation and heating of different elements in the accelerator ring. In particular, power deposition in the kicker magnets can be a limitation: if the temperature of the ferrite yoke exceeds the Curie temperature, the beam will not be properly deflected. In addition, the imaginary portion of the beam coupling impedance contributes to beam instabilities. A good knowledge of electromagnetic properties of materials up to GHz frequency range is essential for a correct impedance evaluation. This paper presents the results of transmission line measurements of complex initial permeability and permittivity for different ferrite types. We present an approach for deriving electromagnetic properties as a function of both frequency and temperature; this information is required for simulating ferrite behaviour under realistic operating conditions.

INTRODUCTION

In circular accelerators, injection and extraction systems place newly injected or extracted particles onto the correct trajectory while aiming to minimize the beam losses. A major component of these systems are fast kicker magnets, which are typically ferrite loaded transmission line type magnets. These magnets consists of multiple cells to approximate a transmission line, where C-shape yokes of magnetic material (typically NiZn ferrites) are sandwiched between high voltage capacitance plates [1]. A key parameter of a ferrite is permeability, which effects the strength and homogeneity of the magnetic field. An accurate model of the ferrite's permeability is critical to understanding its behaviour and for proper beam coupling impedance simulations. The permeability is of particular interest as the ferrite approaches its Curie temperature (T_c).

Beam induced power deposition, due to circulating beam passing through the kicker aperture, can cause an increase in ferrite temperature. More specifically, the power deposition in the ferrite is dependent upon the interaction of the beam spectrum with the real component of the longitudinal beam coupling impedance of the magnet [2]. A change in ferrite properties, due to the beam induced heating, will also influence beam coupling impedance. Importantly, good impedance evaluation is critical, as the impedance can also affect beam stability in the transverse and longitudinal planes [3].

CMD5005 (Ceramic Magnetics, Inc.) [4] or 8C11 (Ferroxcube) [5], both of which have $T_c \geq 125°C$ as indicated by the supplier, are used for the CERN LHC MKI injection, the SPS MKP injection and SPS MKE extraction kicker magnets. A major concern is that beam induced heating of the ferrite yoke will result in severely degraded performance of the kickers, especially during operation with long fills with high beam intensity [6, 7].

Employing an alternative ferrite, e.g. CMD10, that has a higher Curie temperature ($T_c \simeq 250°C$) than CMD5005 and 8C11, in the MKI magnet, was considered [8], but its initial permeability [4] is lower than required for the MKI. As a result, a ferrite of a 50/50 mixture in powder of CMD5005 and CMD10 is being considered, and it will be tested in a prototype SPS MKP kicker magnet [9]. This blended ferrite, CMD10B, will have a higher Curie temperature (190°C expected) than CMD5005 or 8C11 but with higher initial permeability than CMD10. The goal of the current studies is to measure initial permeability as a function of temperature. If the performance of CMD10B is satisfactory, replacement of some of the yokes in the MKI could be considered. An additional note, for NiZn ferrites the permeability data provided by the manufacturer is sometimes only up to 10's of MHz, which is inadequate for beam coupling impedance simulations (GHz range required). The electromagnetic properties of ferrites CMD5005, CMD10 and CMD10B are presented here as a function of both frequency and temperature.

ELECTROMAGNETIC CHARACTERIZATION OF MATERIALS

The response of a material to an applied electromagnetic field is quantified by the material's complex permeability (μ^*) and permittivity (ε^*), which are related to the free space parameters by the relative parameters $\mu^*=\mu_r^*\mu_0$ and $\varepsilon^*=\varepsilon_r^*\varepsilon_0$.

Electromagnetic properties of the materials can be determined using coaxial line measurement methods. A sample of the ferrite is placed within a 50 Ω coaxial line test fixture (see Fig. 1) and S-parameters are measured using a vector network analyzer (VNA) [10]. At the sample's position within the line, the cross section of the line should be completely and homogeneously filled by the sample: however small air gaps cannot be avoided. The material properties are extracted from the measured S-parameters using algorithms, which are presented in the following sections. This paper focuses on two different non-resonant measurements: transmission and short-circuit line methods.

* agnieszka.chmielinska@cern.ch

ISBN: 978-3-95450-184-7 doi:10.18429/JACoW-IPAC2018-WEPMF089

Figure 1: Coaxial line test fixture with Dezifix connector [10], PT100 sensor, heating braid and non-reversible temperature indicators.

Transmission Method

The transmission method [11] allows for simultaneous measurement of μ_r^* and ε_r^*. A toroidal sample of length d loads a section of transmission line, that has a length $L = L_1 + L_2 + d$ (see Fig. 2). If Z_0 is the characteristic impedance of the transmission line and $k_0 = \omega\sqrt{\mu_0\varepsilon_0}$ is the propagation constant in the free-space region, then in the ferrite loaded region: $Z = Z_0\sqrt{\frac{\mu_r^*}{\varepsilon_r^*}}$ and $k = k_0\sqrt{\mu_r^*\varepsilon_r^*}$. The reflection coefficient at material boundaries is $R = \pm\frac{Z-Z_0}{Z+Z_0}$.

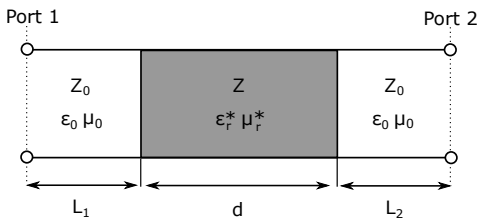

Figure 2: Simplified diagram of the measurement setup.

The expressions for μ_r^* and ε_r^* for this method are given by:

$$\varepsilon_r^* = \varepsilon_r^{'} - j\varepsilon_r^{''} = \frac{k}{k_0}\left(\frac{1-R}{1+R}\right) \tag{1}$$

$$\mu_r^* = \mu_r^{'} - j\mu_r^{''} = \frac{k}{k_0}\left(\frac{1+R}{1-R}\right) \tag{2}$$

where a single-prime and double-prime donates the real and imaginary components, respectively. R and k are derived from measured S-parameters:

$$k = \frac{1}{d}cos^{-1}\left(\frac{e^{-j2k_0(L_1+L_2)} + S_{21}^2 - S_{11}^2}{2e^{-jk_0(L_1+L_2)}S_{21}}\right) \tag{3}$$

$$R = \frac{S_{11}}{e^{-jk_0(L_1+L_2)} - S_{21}e^{-jkd}} \tag{4}$$

Short-Circuit Line Method

If, in Fig. 2, L_2=0 and a short-circuit is placed on port 2, we have a short circuit line method [10, 12]. Since only S_{11} is measured and the sample is placed against a short-circuit, only μ_r^* is extracted and ε_r^* must be known. In this study, ε_r^*=12 is used, which was given in the datasheet [4] and was confirmed by the results of the transmission line measurement method (see below). $S_{11filled}$ and $S_{11empty}$ are the measured S-parameters of the filled and empty sample holder, respectively. The following equation, shown in [12], is solved for μ_r^* using the Newton-Raphson algorithm:

$$\frac{S11_{filled}}{S11_{empty}} + e^{j2k_0L_1}\frac{\tanh(k_0\sqrt{\mu_r^*\varepsilon_r^*}L_1) - \sqrt{\frac{\varepsilon_r^*}{\mu_r^*}}}{\tanh(k_0\sqrt{\mu_r^*\varepsilon_r^*}L_1) + \sqrt{\frac{\varepsilon_r^*}{\mu_r^*}}} = 0 \tag{5}$$

RESULTS

Measurements at Room Temperature

The μ_r^* and ε_r^* have been derived from the transmission method performed at 25°C. Figure 3 shows $\varepsilon_r^{'}$ for three types of ferrite: there is a good agreement with the expected value of $\varepsilon_r^* \in (12-13)$ [4, 13] for frequencies above 400 MHz.

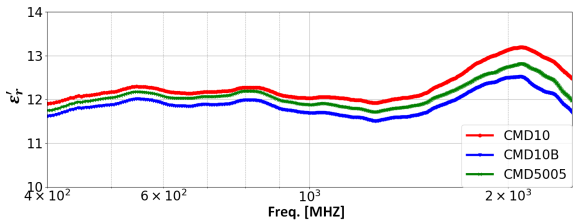

Figure 3: $\varepsilon_r^{'}$ for three types of ferrites at 25°C.

Figure 4 shows μ_r^* for CMD5005 ferrite: there is good agreement between the two measurement methods and the datasheet [4]. However, since the transmission line method is more prone to error at higher frequencies, the short-circuit line technique was predominantly used in these studies.

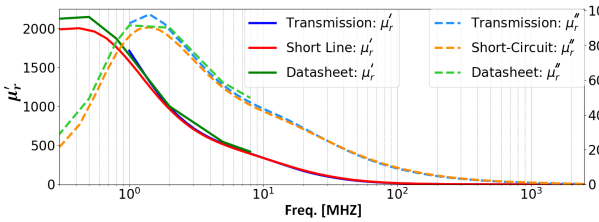

Figure 4: μ_r^* of CMD5005 ferrite at 25°C.

Figures 5 and 6 show $\mu_r^{'}$ and $\mu_r^{''}$, respectively, for the three ferrite types, measured using the short-circuit line method. The maximum measured frequency is limited by the half-wavelength resonance [12]. In repeated measurements it has been observed that $\mu_r^{'}$ oscillates around zero at high frequencies: this effect requires further investigation. Since CMD10B is a 50/50 blend of CMD10 and CMD5005, its μ_r^* is in between those of these ferrites, as expected. Below 100 MHz the $\mu_r^{''}$ of the three ferrites is quite different.

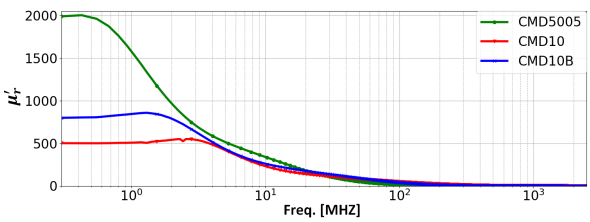

Figure 5: Measured $\mu_r^{'}$ of ferrites at 25°C.

ISBN: 978-3-95450-184-7 doi:10.18429/JACoW-IPAC2018-WEPMF089

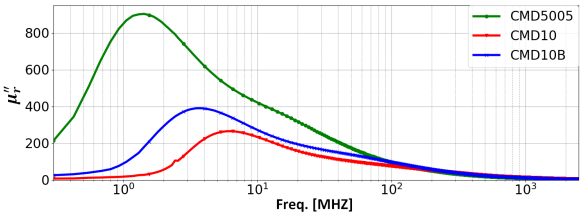

Figure 6: Measured μ_r'' of ferrites at 25°C.

Heated Sample Measurements

Heated sample measurements were performed using a power supply powering a heating braid that was wrapped around the coaxial line test fixture (Fig. 1). The required temperature was set and the output of the supply was controlled by feedback from a temperature sensor. As a cross-check on the temperature, a PT100 sensor and non-reversible temperature indicators were used on the outside of the sample holder. However it was not possible to measure the temperature of the ferrite sample directly. Hence, temperatures shown in this paper are those set, i.e. on the outside of the test fixture: the ferrite sample would be cooler than, because of thermal conduction via the cables to the VNA. The set temperature was increased in steps, ensuring thermal equilibrium of the sample was reached at each step by monitoring the stability of the S-parameters, before the S-parameters were recorded.

To prevent damage to the test fixture, measurements were limited to T_{max}=175°C, therefore only the CMD5005 reached its Curie temperature, indicating that the ferrite CMD5005 was above ~125°C; Figs. 7 and 8 show μ_r' and μ_r'', respectively. At 150°C set, the CMD5005 was still below its Curie temperature (~125°C). Below ~10 MHz, μ_r^* generally increases with temperature, while at higher frequencies the opposite effect is observed. Hence, two mechanisms of losses can be distinguished in the μ_r^* spectra: resonance-type for domain wall motion and relaxation-type for the spin rotation [14, 15]. Above $T_C \geq 125$°C, μ_r' and μ_r'' are both significantly reduced: the ferrite is magnetically nearly transparent and lossless.

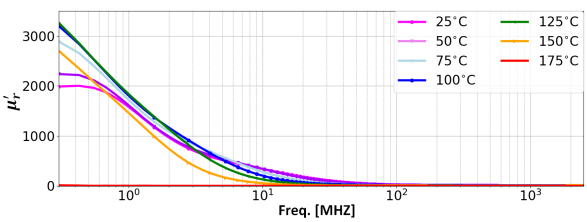

Figure 7: Temperature dependence of μ_r' for CMD5005.

The LHC beam bunches are typically spaced by 25 ns: this results in line harmonics at multiples of 40 MHz, which can significantly contribute to power deposition in the ferrite. The results show that, above 40 MHz, μ_r'' decreases with increasing ferrite temperature: for a given beam, this would result in a reduction in beam induced power deposition as the ferrite heats up. This reduction in beam induced power deposition is not presently accounted for and thus losses

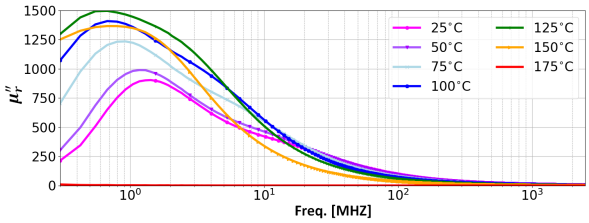

Figure 8: Temperature dependence of μ_r'' for CMD5005.

are overestimated at higher temperatures. Hence, dedicated simulations will also be run at higher temperatures [16]

An interesting analysis is the comparison of μ_r^* for all ferrites at higher temperatures. At frequencies below ~10 MHz, which is the highest significant frequency in a pulse with 30 ns rise-time, μ_r' must be above 500 to provide the required field strength for the MKI [17]. However at 50°C set μ_r' is 300, for CMD5005, at 10 MHz (Fig. 7), and is less than 100 at 150°C set (Fig. 9). For both CMD10 and CMD10B μ_r' is ~300 at 150°C set (Fig. 9). For the LHC MKI, the homogeneity of the field stays within specification when the relative permeability is above 100 up to 10 MHz [17]. This condition is satisfied, unless the operating temperature of CMD5005 reaches its Curie point.

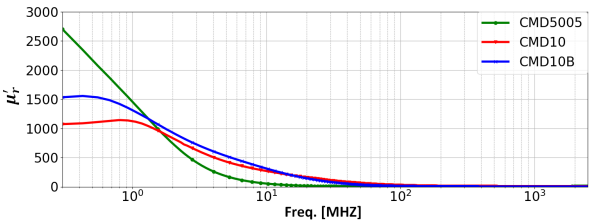

Figure 9: μ_r' at 150°C set, for the three types of ferrites.

CONCLUSIONS

The electromagnetic properties of CMD5005, CMD10 and CMD10B ferrites have been successfully characterized, into the GHz range, using transmission and short circuit measurement methods. A good agreement between the two methods, as well as the available low frequency data from the manufacturer, has been achieved for the CMD5005. The results are important both for understanding the μ_r^* of ferrites and for the accurate simulation of beam coupling impedance.

It is also necessary to have accurate μ_r^* data for ferrites as a function of temperature, especially approaching and exceeding the Curie point: this can occur with high intensity beam circulating for many hours. A comparison of the properties of the three types of ferrite shows that a new type, CMD10B, maintains its initial μ_r', at 10 MHz, to higher temperatures than CMD5005. The presented results also show that, above 40 MHz, μ_r'' decreases with increasing ferrite temperature: for a given beam, this would result in a reduction in beam induced power deposition as the ferrite heats up. Hence, the measurement results at 25°C and at higher temperature are vital input for beam coupling impedance simulations and to understand kicker magnet ferrite yoke behaviour.

ISBN: 978-3-95450-184-7 doi:10.18429/JACoW-IPAC2018-WEPMF089

REFERENCES

[1] M. J. Barnes, L. Ducimetière, T. Fowler, V. Senaj, L. Sermeus, "Injection and extraction magnets: kicker magnets", CERN, Geneva, Switzerland, Rep. CERN-2010-004, March 2011, pp. 141-166.

[2] A. Chmielińska *et al.*, "Preliminary estimate of beam induced power deposition in a FCC-hh injection kicker magnet", in *Proc. IPAC'17*, Copenhagen, Denmark, May 2017, paper WEPVA095, pp. 3475-3477.

[3] A. W. Chao, "Physics of collective beam instabilities in high-energy accelerators", New York, USA: John Wiley and Sons, 1993.

[4] National Magnetics Group, http://www.magneticsgroup.com

[5] Ferroxcube, https://www.ferroxcube.com

[6] V. Vlachodimitropoulos, M. J. Barnes, L. Ducimetière, L. Vega Cid, W. Weterings, "Study of an Improved Beam Screen Design for the LHC Injection Kicker Magnet for HL-LHC", in *Proc. IPAC'16*, Busan, Korea, May 2016, paper THPMW030, pp. 3471-3474.

[7] M. J. Barnes *et al.*, "Studies of Impedance-Related Improvements of the SPS Injection Kicker System", in *Proc. IPAC'17*, Copenhagen, Denmark, May 2017, paper WEPVA094, pp. 3471-3474.

[8] M. J. Barnes, L. Ducimetière, N. Garrel, B. Goddard V. Mertens, W. Weterings, "Analysis of Ferrite Heating of the LHC Injection Kickers and Proposals for Future Reduction of Temperature", in *Proc. IPAC'12*, New Orleans, Louisiana, USA, 20-25 May 2012, paper TUPPR090, pp. 2038-2040.

[9] M. J. Barnes, L. Ducimetière, L. Sermeus, W. Weterings, "Discussion: Baseline, Mid-term and Long-term Strategy for MKP-L", MKP Strategy Meeting, CERN, Geneva, Switzerland, June 28th, 2017.

[10] C. Vollinger, F. Caspers, E. Jensen, "Permittivity and Permeability Measurement Methods for Particle Accelerator Related Materials", in *Proc. IPAC'14*, Dresden, Germany, July 2014, paper THPRI054, pp. 3893-3895.

[11] W. Barry, "A Broad-Band, Automated, Stripline Technique for the Simultaneous Measurement of Complex Permittivity and Permeability", *IEEE Transactions on Microwave Theory and Techniques*, vol. 34, no. 1, p. 80, January 1986.

[12] J. Baker-Jarvis, M. D. Janezic, J. H. Grosvenor, and R. G. Geyer, "Transmission/reflection and short-circuit line methods for measuring permittivity and permeability", NIST, Gaithersburg, MD, USA, Tech. Rep. 1355, March 1993.

[13] J. A. Dinkel, C. C. Jensen, "Comparison of Ferrite Materials for Pulse Applications", in *Proc. 9th IEEE Pulsed Power Conference*, Albuquerque, New Mexico, June 21-23, 1993.

[14] F. Fiorillo , C. Beatrice , M. Coisson, L. Zhemchuzhna, "Loss and Permeability Dependence on Temperature in Soft Ferrites", *IEEE Transactions on Magnetics*, vol. 45, no. 10, p. 4242, October 2009.

[15] T. Tsutaoka, T. Kasagi, T. Nakamura, K. Hatakeyama, "High Frequency Permeability of Mn-Zn Ferrite and its Composite Materials", *J. Phys. IV France*, vol. 7, no. C1, p. 557, March 1997.

[16] V. Vlachodimitropoulos, M. J. Barnes, A. Chmielińska, "Approaches to Extracting Beam Induced RF Power in the LHC Injection Kicker Magnet", presented at IPAC'18, Vancouver, Canada, April 2018.

[17] M. J. Barnes, L. Ducimetière, "Vacuum, Ferrite, Cooling, Beam Impedance and Pre-Scrubbing", 3rd MKI Strategy Meeting, CERN, Geneva, Switzerland, February 20th, 2012.